ARTICLE INFO

Keywords:
Lung cancer
Chronic Obstructive Pulmonary Disease
Proteomics
Biomarker
Mass spectrometry
Diagnosis

ABSTRACT

Lung cancer, COPD and cardiovascular diseases are highlighted as some of the most common disease that cause mortality, and for that reason are the most active areas for drug development. This perspective paper overviews the urgent need to develop a health care system for a rapidly growing patient population in Japan, including forthcoming demands on clinical care, expecting outcomes, and economics. There is an increasing requirement to build on the strengths of the current health care system, thereby delivering urgent solutions for the future. There is also a declaration from the Ministry of Health, Labour and Welfare (MHLW), to develop new biomarker diagnostics, which is intended for patient stratification, aiding in diagnostic phenotype selection for responders to drug treatment of Japanese patients.

This perspective was written by the panel in order to introduce novel technologies and diagnostic capabilities with successful implementation. The next generation of personalized drugs for targeted and stratified patient treatment will soon be available in major disease areas such as, lifestyle-related cancers, especially lung cancers with the highest mortality including a predisposing disorder chronic obstructive pulmonary disease, cardiovascular disease, and other diseases. Mass spectrometric technologies can provide the "phenotypic fingerprint" required for the concept of Personalized Medicine. Mass spectrometry-driven target biomarker diagnoses in combination with high resolution computed tomography can provide a critical pathway initiative facilitated by a fully integrated e-Health infrastructure system.We strongly recommend integrating validated biomarkers based on clinical proteomics, and medical imaging with clinical care strategy supported by e-Health model. This will help to create personalized treatment paradigms and to reduce mortality and healthcare costs of chronic and co-morbid diseases in the elderly population of Japan.

Contents

1. Japanese health care

The elderly population (above 65 years of age) in Japan is currently 21% (27.4 million) reaching 25.2% by 2020, and 40% by 2055. The estimated doubling time (from 7% to 14%) of the 65 and older population is calculated to be 26 years, compared to a 75-year doubling time in the US, and presents a unique demographic shift toward an aging population. In comparison to other countries, Japan is unique, with an overwhelming number of elderly population, which is close to 40%, as predicted by 2050. This should be compared to the US, where the prediction of the transition of elderly population is at about the half, 20%. These data on long-term transition of elderly population rate in eight countries have been published recently (2009) by the National Institute of Population and Social Security Research. There is a general global trend of an increase of the elderly population. The comparative predictions of the elderly age group for Japan in-between 2010 and four decades ahead (until 2050) is an increase of 60%, as illustrated in Fig. 1. The data also predict that with a perspective of a century the increase of the elderly population in Japanese society is expected to grow with 100%, which is remarkable. As a general global trend, the elderly population is growing with varying speed in the respective countries.

Currently, Japan has a low cost functional system with the current healthcare costs accounting for 8.5% of GDP (or nearly 2100 US$ per capita), including 85% contribution by public

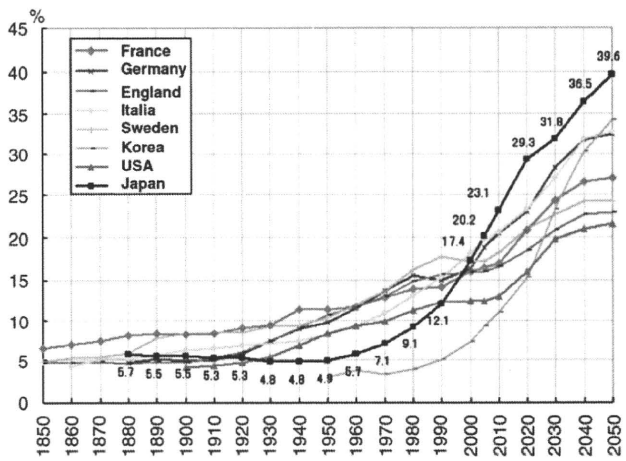

Fig. 1 – A prominent demographic shift toward the elderly population in Japan. The ordinate indicates the percent of the 65 and older population.

Please cite this article as: Kato H, et al, Developments for a growing Japanese patient population: Facilitating new technologies for future health care, J Prot (2011), doi:10.1016/j.jprot.2010.12.006

funds. However, the change in elderly population demographics will create increased demand on the healthcare system, thereby requiring for innovations in healthcare and treatment.

With the elder population expanding, the lifestyle-related cancer rates will inevitably increase. Smoking-related lung cancer's mortality has already been the highest among all cancers in both Japan and United States. Chronic obstructive pulmonary disease (COPD) is another tobacco- or air pollution-related disease, and can predispose patients to lung cancers. Japan is the world's largest market for tobacco products (smoking rate at 29%) and has COPD prevalence estimates similar to western countries with over 5 million COPD patients [1]. The cost impacts of COPD in Japan have been huge and estimated at 805.5 billion ¥ (6.8 billion US$) per year; 645.1 billion ¥ (5.5 billion US$) in direct costs and 160.4 billion ¥ (1.4 billion US$) in indirect costs (direct and indirect costs are split as 80% to 20%). COPD is a preventable disease with cessation of smoking, which has widely been promoted to reduce the prevalence of the disease; it will take longer time for the promotion to become indeed effective. Given its complexity and the long term effects of smoking, COPD requires early detection and therapeutic evaluation with comprehensive multi-modalities, and further detection and management of co-morbidities (such as lung cancer and heart disease) that modify outcomes of the primary disease [2,3]. Lung cancer is a "multifactorial" disease, *i.e.*, many factors work together to cause the disease. Most lung cancer patients actually have COPD with progressed emphysema and infectious disease agents such as *Chlamydia pneumoniae*, human papilloma virus (HPV) and measles [4–6]. Possibly, these factors in combination with certain genetic changes may be the initial cause of lung cancer. Researchers are now beginning to isolate some of the genomic factors that are associated with an increased risk of lung cancer. Paradoxically, the incidences of chronic heart disease (CHD) and atherosclerosis in Japan have been in decline. This may be attributed to lower serum cholesterol, declining rates of smoking and declining trends in blood pressure [7]. However, CHD continues to be a major cause of death in smokers with different co-morbidities. A number of studies in Japan have shown that smoking increases the risk of premature death among both men and women. In conclusion, it is likely that environmental factors, in addition to organic cooking (mostly in Asian countries), as well as occupational reasons in addition to smoking are risk factors that contribute to the development of cancer and CHD. Thus, the smoking effects are the major factors for these diseases.

Currently there are 109 unique protein biomarkers used daily in the clinic [8,9]. There are limited studies available for biomarker of diseases except some of the cancer biomarkers until today. Examples like; human epidermal growth factor receptor 2 (HER2), KL6, SA100, prostate specific antigen (PSA) and creatine phosphokinase (CPK) are some markers that are used globally today.

Within lung cancer, there have been reports on early indication of somatic mutation appearances within the EGF receptor. The increased mutation frequency was observed especially in Japan and Asia [10]. The Japanese lung cancer patients showed to have a certain percentage of non-responders, the reason for this was not well understood at the time. At a later time point, when the number of Gefiinib (IRESSA) treated patients increased to tens of thousands, the mutations within the EGF-receptor was discovered at high frequencies [8,11–13]. Later, these somatic mutations were shown to have a direct link to the specific inhibitory effects of IRESSA. Today, an EGFR-mutation assay outcome will guide the clinicians in Japan, to what treatment and medication to use for these patients. Epidermal growth factor receptor is associated to resistance to chemotherapy as has been the case with radiation therapy. The restricted treatment efficacy opened up for novel drugs such as Gefitinib and Erlotinib, developed as specific EGFR-tyrosine kinase inhibitors (TKI), with good efficacy and less side effects. A recent study also presented the situation in Europe [14].

It is evident in Asian populations that the majority of the non-small cell lung cancer (NSCLC) patients with activated mutations achieved a durable and effective response to EGFR TKI-treatment, such as Gefitinib [15,16].

The somatic mutation assay test has now been put into place in Japan, and is used routinely to identify the various lung cancer phenotypes. In addition, a large case–control study was conducted in Japan, involving 52 clinical centers throughout Japan. This epidemiological study was also directed towards biomarker discovery and probably makes it the biggest clinical Biomarker Discovery study undertaken within the industry [17,18].

The future medical treatment of patients is expected to have an increased need to combine diagnosis such as imaging and biomarkers with selection of drug prescriptions for patients. These expected developments are currently being assessed by the FDA and NIH, in collaborative programs and studies with the Pharma industry.

To address the future challenges that Japanese society is facing, novel technologies and diagnostic capabilities must be developed and implemented throughout the coming decade. It is steadily advancing to discover novel target biomarkers that are directly related to pathophysiology and etiology, and to develop diagnostic strategies with those markers. Imaging modalities including high resolution computer tomography (HRCT), magnetic resonance imaging (MRI) and positron emission tomography (PET) have been commonly used for diagnosis in average Japanese hospitals and even in health-care clinics. However, these proteomic and imaging methods are now being used separately and provide mutually independent information. COPD involves multiple compartments in the lung, such as the airways, parenchyma, as well as vessels, and causes remodelling and destruction, which can vary among individuals. The genetic basis for such a difference in susceptibility and disease presentation is currently being elucidated and potential genes implicated are currently validated [19]. CT offers a non-invasive approach to image COPD disease changes [20] at a spatial resolution of 0.5 mm in X and Y directions and 1 mm in Z direction which helps in accurately resolving changes in airways of around 2 mm [21]. However, additional novel techniques like optical coherence tomography (OCT) can provide a spatial resolution of around 3 to 16 μm and an ability to image at a surface depth

Please cite this article as: Kato H, et al, Developments for a growing Japanese patient population: Facilitating new technologies for future health care, J Prot (2011), doi:10.1016/j.jprot.2010.12.006

of 3 mm [22]. Currently, new developments are progressing where the combination of HRCT imaging and target biomarker expression analysis may assess a correlation between histopathological changes and biomarker levels. This interdisciplinary approach will help to identify disease at an early stage and the degree of progression, and thus to improve an individual patient's outcome. Upon drug treatment, changes in the CT-image and biomarker assay read-outs will indicate outcomes for the patient. The ultimate goal would be to monitor the treatment response in clinical and functional variables that show good correlation to CT measurements with HRCT, with less variability than the placebo group.

Another important consideration, which remains as a top priority for future Personalized Medicine developments, is the drugs with low frequency of adverse events. Patient safety, which relates to the minimization of side effects, is crucial in order to limit the suffering of patients, as an effect of drug use.

Japan has declared a pricing strategy that includes request for new biomarker diagnostics that can be used for patient stratification, with phenotype selection for responders to drug treatment [23]. In this declaration, pharmaco-genomic, and proteomic technologies are promoted in the discovery and development of drug related biomarkers by the drug pricing committee within the Ministry of Health, Labour and Welfare (MHLW), (http://www.mhlw.go.jp/shingi/2009/07/dl/s0715-9a.pdf).

The pricing strategy will be used in order to promote safe and efficient approved drugs for the treatment of Japanese patients.

2. Protein biomarker diagnosis

Detection of new biomarkers of emphysema and inflammatory reaction in the lung and heart can aid in early identification of disease and in monitoring the effect of therapeutic agents on disease progression. There is currently much research activity in this area but no consensus regarding which bio-molecules are most useful for the identification of COPD progression or for predicting clinical outcomes.

It is expected that multiplexed biomarker assay platforms will play an important clinical role as becoming a complement to traditional immuno-assays for future molecular diagnostics. An early evidence of the progress developments is that recently, the interagency group of the National Cancer Institute and the Food and Drug Administration (NCI-FDA) presented the validation of protein based multiplex assay [24]. In addition, they reported on Multiplexed Biomarker Assay Platform developments where the NCI-FDA Oncology Task Force, members of the Clinical Proteomic Technology Assessment for Cancer program, are evaluating both antibody based multiplexing as well as mass spectrometry based MRM assays [25].

Multiplexed biomarker assay platforms are expected to be the key platforms that will help improve the clinical health care, and targeted medication in the future. The mass spectrometry based MRM assay panels would be using the same SRM/MRM principles as for drug and metabolite monitoring. These quantitative multiple reaction monitoring (MRM) methods have been in use for more than a decade in the development of new medicines, and this has been in close collaboration with the FDA.

Currently the available triple-quadrupole mass spectrometers have both improves sensitivity, mass accuracy as well as scan speed that is in line with the multiplex measurement principle.

3. Multiplexed biomarker assay platforms

Mass spectrometry-based selective reaction monitoring is rapidly developing with an expectation to become a preferred technology for the development of quantitative protein or peptide assays with high sensitivity and selectivity for clinical research [26,27]. Its sequential application to multiple targets at once MRM delivers high-throughput, and when taken together, these parameters provide a breakthrough quantification methodology. This technology allows absolute biomarker quantification in very small amounts of bio-fluid samples, allowing multiplexed read-outs of disease panels.

Assay formats with multiple hundreds of proteins/assay have recently been presented [28,29]. It is expected that clinical assay panels with 100 proteins/assay, screening both blood samples and tissues will be standard in laboratories around the world in the near future. The MRM assay format measures specific target proteins by monitoring *proteotypic* (unique to the target protein) peptide sequences. The technology is fully quantitative when isotopically labeled internal standards are included in the assay. No immuno-reagents are required for MRM assays in principle but immuno-precipitation or other affinity enrichment techniques may be used in sample preparation to enhance the sensitivity of the assay. The MRM technology is performed on triple quadrupole mass spectrometers and provides precise quantification and broad dynamic range, even within highly complex sample matrices. The multiplex MRM assays allow high density data generation in clinical diagnosis, where it is envisioned that multiple MRM-panels can be run simultaneously. This would provide a whole new setting, whereby the health care system would perform future patient diagnosis. In fact, immunoassay platforms like ELISA, with extensive robotics and automation would face major difficulties fulfilling these performances. Even with current synthesis technologies of isotope labeled internal standards, it makes MRM-assay costs highly competitive in comparison to current pricing in the clinical hospitals running clinical assays.

In addition, when mass spectrometry is coupled with a front-end sample introduction system such as nano-flow liquid chromatography, the limit of quantification/detection of target peptides/proteins and biomarkers may reach low attomole levels. The utilization of this technology makes analysis of clinical "fingerprint" target biomarkers in common body fluids not only possible, but also an attainable goal for the future. Recent promising efforts to combine MRM with sampling at histological levels [30], will facilitate finding the body fluid targets of which levels correlate with those at disease foci, serving as a diagnostic strategy combined with HRCT. MRM delivers a unique signal that can be detected and quantified in the midst of a very complicated biological matrix. The mass spectrometry spectra plots are simple, usually containing only a single peak for each MRM. This

Please cite this article as: Kato H, et al, Developments for a growing Japanese patient population: Facilitating new technologies for future health care, J Prot (2011), doi:10.1016/j.jprot.2010.12.006

characteristic makes the assay especially suitable for sensitive and specific quantitation [31].

The latest developments within the MRM technology are providing high density assay panels with high sensitivities, allowing low abundant level proteins to be quantified, even down to copy numbers as low as 40 copies/cell [28].

In comparison with ELISA immunoassays, recently MRM panels were presented in blood plasma with linear operational performance down to low pg/ml [24].

Imaging using CT, MRI, ultrasound, molecular imaging is commonly used in clinical practice and also in therapeutic trails. They help in non-invasively quantifying regional disease, which is critical for validating clinical proteomic biomarkers elucidated from different tissue compartments.

Computed tomography (CT) is considered a novel modality to estimate the key pathological changes in COPD patients, namely emphysema and airway remodeling. Japan is in the forefront of CT technology and has access to the advanced scanner hardware and required expertise in radiology and informatics. CT offers a non-invasive approach to image COPD disease changes [20] at a spatial resolution of 0.5 mm in X and Y directions and 1 mm in the Z direction which helps in accurately resolving changes in airways of around 2 mm [21]. By accurate quantification of the disease pathology CT allows phenotyping (or patient stratification) for evaluating novel treatments or determining prognoses. Several academic groups and large chest radiology consortia like the Fleischner Society (www.fleischner.org/) continue to bring novel insights into the application of CT technology and standardization of the method for evaluating COPD and the Big3 diseases, *i.e.*, "lung cancer", "COPD" and "atherosclerosis". By using automated CAD tools in batch mode, image analysis and quantification can be done in high-throughput allowing application to large-scale databases.

However, in addition novel techniques like optical coherence tomography (OCT) can provide a spatial resolution of around 3 to 16 μm and an ability to image at a surface depth of 3 mm [22]. MRI imaging using hyperpolarized gases like helium, xenon and fluoride and molecular imaging with PET offer exciting insights into functional status.

Lung cancer imaging using CT together with PET for imaging the volume and functional status of lung nodules is widely used in clinical setting. These tools are used in screening of large cohorts of smokers and currently the benefits of screening are being evaluated. Together with tumor based proteomic biomarkers, imaging offers strong model to related function, structure and disease stage with proteomic finger print, thereby supporting the validation of clinical proteomic endpoints in smoking related lung diseases. In addition, a large part of the lung cancer patients with diagnosed tumors, also show radiological evidence of emphysema and airway disease [32,33].

Critical path initiative (CPI) is the US national strategy for transforming the way FDA-regulated products are developed, evaluated, manufactured, and used with a focus on accelerating the development of safe and efficacious novel treatments (http://www.fda.gov/ScienceResearch/SpecialTopics/CriticalPathInitiative/default.htm). CPI has initiated several opportunities centered around the development and validation of novel biomarkers for smoking-related diseases including soluble biomarkers, patient-reported outcomes and imaging. NHLBI/NIH has initiated a program for Sub Populations and InteRmediate Outcome Measures In COPD (SPIROMICS), which focuses on combining biomarkers and imaging endpoints for outcome assessment in COPD patients.

In *eHealth developments*, the exchange of health information electronically between physicians, hospitals, health plans, and patients has increased substantially in the last year and is reducing the cost of care and positively impacting physicians, according to a new survey released by the non-profit eHealth Initiative (eHI) today. "Migrating Toward Meaningful Use: The State of Health Information Exchange," a report based on eHI's *Sixth Annual Survey of Health Information Exchange*, presents a very clear benefit to the health care system. Responses from operational initiatives demonstrate an increasingly positive impact on the efficiency of care while showing a return on investment.

Acknowledgements

This study was supported by a joint grant from the Swedish Research Council, Vinnova, SSF, under the program Biomedical Engineering for Better Health.

REFERENCES

[1] Fukuchi Y, Nishimura M, Ichinose M, Adachi M, Nagai A, Kuriyama T, et al. COPD in Japan: the Nippon COPD Epidemiology Study. Respirology 2004;9:458–65.
[2] Fabbri LM, Rabe KF. From COPD to chronic systemic inflammatory syndrome? Lancet 2007;370:797–9.
[3] Holguin F, Folch E, Redd SC, Mannino DA. Comorbidity and mortality in COPD-related hospitalizations in the United States, 1979 to 2001. Chest 2005;128:2005–11.
[4] Chaturvedi AK, Gaydos CA, Agreda P, Holden JP, Chatterjee N, Goedert JJ, et al. *Chlamydia pneumoniae* infection and risk for lung cancer. Cancer Epidemiol Biomark Prev 2010;19:1498–505.
[5] Simen-Kapeu A, Surcel HM, Koskela P, Pukkala E, Lehtinen M. Lack of association between human papillomavirus type 16 and 18 infections and female lung cancer. Cancer Epidemiol Biomark Prev 2010;19:1879–81.
[6] Sion-Vardy N, Lasarov I, Delgado B, Gopas J, Benharroch D, Ariad S. Measles virus: evidence for association with lung cancer. Exp Lung Res 2009;35:701–12.
[7] Ueshima H. Explanation for the Japanese paradox: prevention of increase in coronary heart disease and reduction in stroke. J Atheroscler Thromb 2007;14:278–86.
[8] Anderson NL. The clinical plasma proteome: a survey of clinical assays for proteins in plasma and serum. Clin Chem 2010;56:177–85.
[9] Anderson NG. Adventures in clinical chemistry and proteomics: a personal account. Clin Chem 2010;56:154–60.
[10] Mok TS, Wu YL, Thongprasert S, Yang CH, Chu DT, Saijo N, et al. Gefitinib or carboplatin–paclitaxel in pulmonary adenocarcinoma. New Eng J Med 2009;361:947–57.
[11] Pao W, Miller V, Zakowski M, Doherty J, Politi K, Sarkaria I, et al. EGF receptor gene mutations are common in lung cancers from "never smokers" and are associated with sensitivity of tumors to gefitinib and erlotinib. Proc Natl Acad Sci USA 2004;101:13306–11.
[12] Ji HB. Mechanistic insights into acquired drug resistance in epidermal growth factor receptor mutation-targeted lung cancer therapy. Cancer Sci 2010;101:1933–8.

Please cite this article as: Kato H, et al, Developments for a growing Japanese patient population: Facilitating new technologies for future health care, J Prot (2011), doi:10.1016/j.jprot.2010.12.006

[13] Sakaeda T, Okamura N, Gotoh A, Shirakawa T, Terao S, Morioka M, et al. EGFR mRNA is upregulated, but somatic mutations of the gene are hardly found in renal cell carcinoma in Japanese patients. Pharm Res 2005;22:1757–61.
[14] Rosell R, Moran T, Queralt C, Porta R, Cardenal F, Camps C, et al. Screening for epidermal growth factor receptor mutations in lung cancer. New Eng J Med 2009;361:958–67.
[15] Inoue A, Saijo Y, Maemondo M, Gomi K, Tokue Y, Kimura Y, et al. Severe acute interstitial pneumonia and gefitinib. Lancet 2003;361:137–9.
[16] Potti A, Mukherjee S, Petersen R, Dressman HK, Bild A, Koontz J, et al. A genomic strategy to refine prognosis in early-stage non-small-cell lung cancer. New Eng J Med 2006;355:570–80.
[17] Kudoh S, Kato H, Nishiwaki Y, Fukuoka M, Nakata K, Ichinose Y, et al. Interstitial lung disease in Japanese patients with lung cancer — a cohort and nested case–control study. Am J Respir Crit Care Med 2008;177:1348–57.
[18] Marko-Varga G, Ogiwara A, Nishimura T, Kawamura T, Fujii K, Kawakami T, et al. Personalized medicine and proteomics: lessons from non-small cell lung cancer. J Proteome Res 2007;6:2925–35.
[19] Baur F, Beattie D, Beer D, Bentley D, Bradley M, Bruce I, et al. The identification of indacaterol as an ultralong-acting inhaled beta(2)-adrenoceptor agonist. J Med Chem 2010;53: 3675–84.
[20] Coxson HO, Rogers RM. Quantitative computed tomography of chronic obstructive pulmonary disease. Acad Radiol 2005;12:1457–63.
[21] Coxson HO, Lam S. Quantitative assessment of the airway wall using computed tomography and optical coherence tomography. Proc Am Thorac Soc 2009;6:439–43.
[22] Fujimoto JG. Optical coherence tomography for ultrahigh resolution in vivo imaging. Nat Biotechnol 2003;21:1361–7.
[23] Committee declaration of the drug pricing within the Ministry of Health, Labour and Welfare (MHLW), Chu-i-kyo, Yaku-1 (July 15, 2009); 2009. p. 1–4. Japanese.
[24] Rodriguez H, Tezak Z, Mesri M, Carr SA, Liebler DC, Fisher SJ, et al. Analytical validation of protein-based multiplex assays: a workshop report by the NCI-FDA interagency oncology task force on molecular diagnostics. Clin Chem 2010;56:237–43.
[25] Regnier FE, Skates SJ, Mesri M, Rodriguez H, Tezak Z, Kondratovich MV, et al. Protein-based multiplex assays: mock presubmissions to the US Food and Drug Administration. Clin Chem 2010;56:165–71.
[26] Gstaiger M, Aebersold R. Applying mass spectrometry-based proteomics to genetics, genomics and network biology. Nat Rev Genet 2009;10:617–27.
[27] Végvári Á, Marko-Varga G. Clinical protein science and bioanalytical mass spectrometry with an emphasis on lung cancer. Chem Rev 2010;110:3278–98.
[28] Picotti P, Bodenmiller B, Mueller LN, Domon B, Aebersold R. Full dynamic range proteome analysis of *S. cerevisiae* by targeted proteomics. Cell 2009;138:795–806.
[29] Picotti P, Rinner O, Stallmach R, Dautel F, Farrah T, Domon B, et al. High-throughput generation of selected reaction-monitoring assays for proteins and proteomes. Nat Meth 2010;7:43–6.
[30] Nishimura T, Nomura M, Tojo H, Hamasaki H, Fukuda T, Fujii K, et al. Proteomic analysis of laser-microdissected paraffin-embedded tissues: (2) MRM assay for stage-related proteins upon non-metastatic lung adenocarcinoma. J Proteomics 2010;76:1100–10.
[31] Huttenhain R, Malmström J, Picotti P, Aebersold R. Perspectives of targeted mass spectrometry for protein biomarker verification. Curr Opin Chem Biol 2009;13:518–25.
[32] Wilson DO, Weissfeld JL, Balkan A, Schragin JG, Fuhrman CR, Fisher SN, et al. Association of radiographic emphysema and airflow obstruction with lung cancer. Am J Respir Crit Care Med 2008;178:738–44.
[33] Kato H, Ikeda N, Yamada T, Nishimura T, Kondo T, Saijo N, Nishio K, Fujimoto J, Nomura M, Oda Y, Lindmark B, Maniwa J, Hibino H, Unno M, Ito T, Sawa Y, Tojo H, Egawa S, Edula G, Lopez M, Wigmore M, Inase N, Yoshizawa Y, Nomura F, Marko-Varga G. Developments for a growing Japanese patient population: facilitating new technologies for future health care. J Proteome Res 2011;9:51–7.

Please cite this article as: Kato H, et al, Developments for a growing Japanese patient population: Facilitating new technologies for future health care, J Prot (2011), doi:10.1016/j.jprot.2010.12.006

DOI:10.1158/1535-7163.MCT-10-0544

Molecular Cancer Therapeutics

Sorafenib Inhibits the Hepatocyte Growth Factor–Mediated Epithelial Mesenchymal Transition in Hepatocellular Carcinoma

Tomoyuki Nagai, Tokuzo Arao, Kazuyuki Furuta, et al.

Mol Cancer Ther 2011;10:169-177. Published online January 10, 2011.

DOI:10.1158/1535-7163.MCT-10-0544

Preclinical Development

Molecular Cancer Therapeutics

Sorafenib Inhibits the Hepatocyte Growth Factor–Mediated Epithelial Mesenchymal Transition in Hepatocellular Carcinoma

Tomoyuki Nagai[1,2], Tokuzo Arao[1], Kazuyuki Furuta[1], Kazuko Sakai[1], Kanae Kudo[1,2], Hiroyasu Kaneda[1], Daisuke Tamura[1], Keiichi Aomatsu[1], Hideharu Kimura[1], Yoshihiko Fujita[1], Kazuko Matsumoto[1], Nagahiro Saijo[3], Masatoshi Kudo[2], and Kazuto Nishio[1]

Abstract

The epithelial mesenchymal transition (EMT) has emerged as a pivotal event in the development of the invasive and metastatic potentials of cancer progression. Sorafenib, a VEGFR inhibitor with activity against RAF kinase, is active against hepatocellular carcinoma (HCC); however, the possible involvement of sorafenib in the EMT remains unclear. Here, we examined the effect of sorafenib on the EMT. Hepatocyte growth factor (HGF) induced EMT-like morphologic changes and the upregulation of SNAI1 and N-cadherin expression. The downregulation of E-cadherin expression in HepG2 and Huh7 HCC cell lines shows that HGF mediates the EMT in HCC. The knockdown of SNAI1 using siRNA canceled the HGF-mediated morphologic changes and cadherin switching, indicating that SNAI1 is required for the HGF-mediated EMT in HCC. Interestingly, sorafenib and the MEK inhibitor U0126 markedly inhibited the HGF-induced morphologic changes, SNAI1 upregulation, and cadherin switching, whereas the PI3 kinase inhibitor wortmannin did not. Collectively, these findings indicate that sorafenib downregulates SNAI1 expression by inhibiting mitogen-activated protein kinase (MAPK) signaling, thereby inhibiting the EMT in HCC cells. In fact, a wound healing and migration assay revealed that sorafenib completely canceled the HGF-mediated cellular migration in HCC cells. In conclusion, we found that sorafenib exerts a potent inhibitory activity against the EMT by inhibiting MAPK signaling and SNAI1 expression in HCC. Our findings may provide a novel insight into the anti-EMT effect of tyrosine kinase inhibitors in cancer cells. *Mol Cancer Ther; 10(1); 169–77. ©2011 AACR.*

Introduction

Hepatocellular carcinoma (HCC) is the fifth most common cancer and the third largest cause of cancer-related death in the world annually (1). Recurrence, metastasis, and the development of new primary tumors are the most common causes of mortality among patients with HCC (2). Sorafenib (Nexavar; Bayer HealthCare Pharmaceuticals Inc.) is a small molecule that inhibits the kinase activities of Raf-1 and B-Raf in addition to VEGFRs, PDGFR-β (platelet-derived growth factor receptor β), Flt-3, and c-KIT (3). Two recent randomized controlled trials reported a clinical benefit of single-agent sorafenib in extending overall survival in both Western and Asian patients with advanced unresectable HCC (4, 5). The potential action mechanisms that lead to these clinical benefits are thought to include antiangiogenic effects and sorafenib's characteristic inhibitory effect on Raf-1 and B-Raf signaling.

Meanwhile, growing evidence indicates that the epithelial mesenchymal transition (EMT), a developmental process by which epithelial cells reduce intercellular adhesions and acquire fibroblastoid properties, has important roles in the development of the invasive and metastatic potentials of cancer progression (6–8). To date, numerous clinicopathologic studies have shown positive correlations between the expressions of the transcription factors SNAI1 (snail homologue 1/SNAIL) and SNAI2 (snail homologue 2/Slug), which are key inducible factors of the EMT, and poor clinical outcomes in breast, ovary, colorectal, and lung cancer; squamous cell carcinoma; melanoma, and HCC (reviewed in ref. 6).

Generally, the activation of a wide variety of ligands including FGF (fibroblast growth factor), TGF-β–BMPs (bone morphogenetic protein), Wnt, EGF (epidermal growth factor), VEGF, and HGF (hepatocyte growth factor) and its receptor can upregulate the expression of EMT-regulating transcription factors, including SNAI1, SNAI2, ZEB1, ZEB2, and TWIST (6). Among them, HGF (also known as scattering factor) activates

Authors' Affiliations: Departments of [1]Genome Biology, [2]Gastroenterology and [3]Medical Oncology, Kinki University School of Medicine, Japan

Note: Supplementary material for this article is available at Molecular Cancer Therapeutics Online (http://mct.aacrjournals.org/).

Corresponding Author: Kazuto Nishio, Department of Genome Biology, Kinki University School of Medicine, 377-2 Ohno-higashi, Osaka-Sayama, Osaka 589-8511, Japan. Phone: 81-72-366-0221 (ext 3150); Fax: 81-72-367-6369; E-mail: knishio@med.kindai.ac.jp

doi: 10.1158/1535-7163.MCT-10-0544

DOI:10.1158/1535-7163.MCT-10-0544

the Met signaling pathway, thereby increasing the invasive and metastatic potentials of the cells and allowing the survival of cancer cells in the bloodstream in the absence of anchorage (9). In addition, HGF is well known as a potent angiogenic cytokine, and Met signal activation can modify the microenvironment to facilitate cancer progression (9). Therefore, the HGF-Met signaling pathway is regarded as a promising therapeutic target, and many molecular targeted drugs are under clinical development (10). In HCC, the mRNA levels of HGF and Met receptor are markedly increased compared with those in normal liver (11). A high serum HGF concentration is associated with a poor prognosis for overall survival after hepatic resection, and the serum level of HGF represents the degree of the carcinogenic state in the livers of patients with C-viral chronic hepatitis and cirrhosis (12–14). Thus, we examined the effect of sorafenib on the HGF-Met–mediated EMT in HCC.

Materials and Methods

Reagents

Sorafenib was provided by Bayer HealthCare Pharmaceuticals Inc. U0126, wortmannin (Cell Signaling Technology), and human HGF (R&D Systems) were purchased from the indicated companies. The structures of compounds are shown in Supplementary Figure 1.

Cell culture

The human HCC cell lines HepG2 and Huh7 were maintained in Dulbecco's modified Eagle's (DMEM) medium (Sigma) supplemented with 10% FBS, penicillin, and streptomycin (Sigma) in a humidified atmosphere of 5% CO_2 at 37°C. The cell lines were obtained from the Japanese Collection of Research Bioresources and were grown in culture for less than 6 months.

Scratch assay

The method used for the scratches assay has been previously described (15). Briefly, the cells were plated onto 24-well plates and incubated in DMEM containing 10% FBS until they reached subconfluence. Scratches were introduced to the subconfluent cell monolayer, using a plastic pipette tip. The cells were then cultured with DMEM containing 10% FBS at 37°C. After 24 hours, the scratch area was photographed using a light microscope (IX71; Olympus). The wound distance between edge to edge were measured and averaged from 5 points per 1 wound area, using DP manager software (Olympus). The 2 wound areas were evaluated in an experiment and the experiment was done in triplicate.

Migration assay

The migration assays were done using the Boyden chamber methods and polycarbonate membranes with an 8-μm pore size (Chemotaxicell), as previously described (15). The membranes were coated with fibronectin on the outer side and dried for 2 hours at room temperature. The cells to be analyzed (2×10^4 cells/well) were then seeded onto the upper chambers with 200 μL of migrating medium (DMEM containing 0.5% FBS), and the upper chambers were placed into the lower chambers of 24-well culture dishes containing 600 μL of DMEM containing 10% FBS or with 10 ng/mL of HGF or with HGF and 10 μmol/L of sorafenib. After incubation for 36 hours (HepG2) and 24 hours (Huh7), the media in the upper chambers were aspirated and the nonmigrated cells on the inner sides of the membranes were removed using a cotton swab. The cells that had migrated to the outer side of the membranes were fixed with 4% paraformaldehyde for 10 minutes, stained with 0.1% Giemsa stain solution for 15 minutes, and then counted using a light microscope. Migrated cells were averaged from 5 fields per 1 chamber and 3 chambers were used on 1 experiment. The experiment was done in triplicate.

Morphologic analysis

HepG2 and Huh7 cells (2×10^4 and 1×10^4 cells/well, respectively) were seeded in 6-well tissue culture dishes. After 24 hours of incubation, the cells were stimulated with 10 ng/mL of HGF or control PBS. When the inhibitors were used, the cells were exposed to each inhibitor for 3 hours before the addition of HGF. After 48 hours, the cells were analyzed using a light microscope. The experiment was done in triplicate.

Western blot analysis

The following antibodies were used in this study: phospho-Met (Y1349), Met, phospho-AKT (S473), AKT, phospho-p44/42 mitogen-activated protein kinase (MAPK), SNAI1/Snail, E-cadherin, N-cadherin, vimentin, β-actin antibody horseradish peroxidase–conjugated secondary antibody (Cell Signaling Technology), and fibronectin (Santa Cruz Biotechnology). All the experiments were done at least in duplicate. The Western blot analysis was done as described previously (16). The data were quantified by automated densitometry using Multigauge Ver. 3.0 (Fujifilm). Densitometric data were normalized by β-actin in triplicate and the average was shown above the Western blot as a ratio of control sample.

Real-time reverse transcription PCR

The real-time reverse transcription PCR (RT-PCR) method has been previously described (17). Briefly, 1 μg of total RNA from the cultured cells was converted to cDNA using a GeneAmp RNA-PCR kit (Applied Biosystems). Real-time RT-PCR amplification was done using a Thermal Cycler Dice (Takara) in accordance with the manufacturer's instructions under the following conditions: 95°C for 6 minutes, 40 cycles of 95°C for 15 seconds, and 60°C for 1 minute. Glyceraldehyde 3-phosphate dehydrogenase (GAPD) was used to normalize the expression levels in the subsequent quantitative analyses. To amplify the target genes, the following primers were purchased from TaKaRa: *CDH1*, forward 5′-TTA AAC

DOI:10.1158/1535-7163.MCT-10-0544

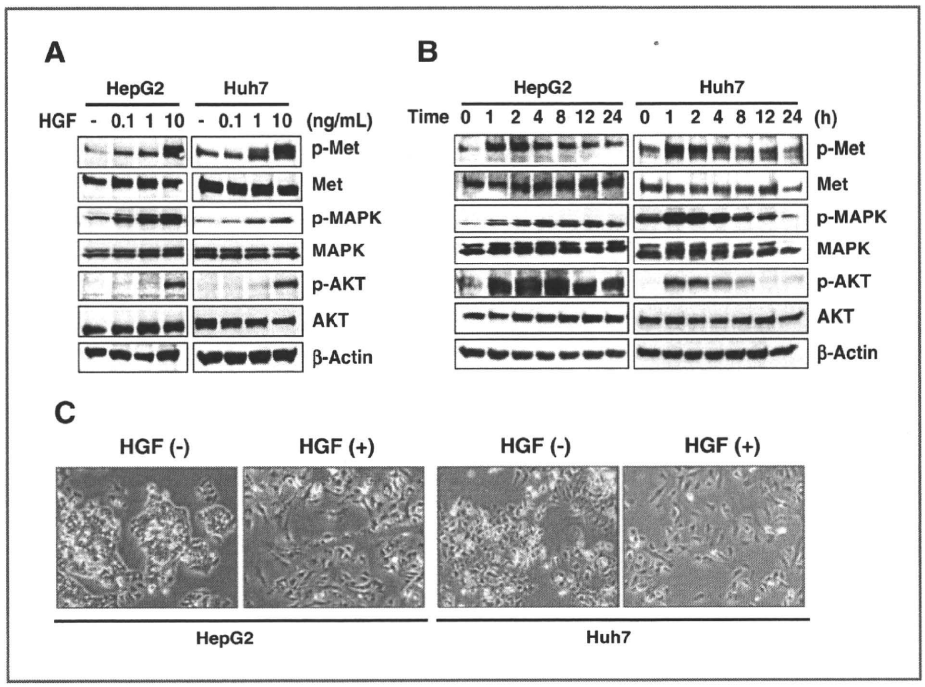

Figure 1. HGF stimulates the Met signaling pathway and induces morphologic changes in HCC. A, HGF stimulation (0, 0.1, 1, and 10 ng/mL) dose-dependently increased the phosphorylation of Met, MAPK, and AKT in the HCC cell lines HepG2 and Huh7. The results of a Western blot analysis are shown. β-Actin was used as a loading control. The serum-starved cells were stimulated with HGF for 60 minutes and then collected for analysis. B, time-course analysis of HGF stimulation. The HCC cells were stimulated with 10 ng/mL of HGF for 0, 1, 2, 4, 8, 12, and 24 hours. The results of a Western blot analysis are shown. C, HGF-mediated morphologic changes included cell scattering and the elongation of the cell shape that are characteristic of the EMT. The HepG2 and Huh7 cells were stimulated with or without 10 ng/mL of HGF for 48 hours and then photographed (magnification × 200).

TCC TGG CCT CAA GCA ATC-3′ and reverse 5′-TCC TAT CTT GGG CAA AGC AAC TG-3′; *CDH2*, forward 5′-CGA ATG GAT GAA AGA CCC ATC C-3′ and reverse 5′-GGA GCC ACT GCC TTC ATA GTC AA-3′; *SNAI1*, forward 5′-TCT AGG CCC TGG CTG CTA CAA-3′ and reverse 5′-ACA TCT GAG TGG GTC TGG AGG TG-3′; *SNAI2*, forward 5′-ATG CAT ATT CGG ACC CAC ACA TTA C-3′ and reverse 5′-AGA TTT GAC CTG TCT GCA AAT GCT C-3′; *VIM*, forward 5′-TGA GTA CCG GAG ACA GGT GCA G-3′ and reverse 5′-TAG CAG CTT CAA CGG CAA AGT TC-3′; *FN1*, forward 5′-GGA GCA AAT GGC ACC GAG ATA-3′ and reverse 5′-GAG CTG CAC ATG TCT TGG GAA C-3′; and *GAPD*, forward 5′-GCA CCG TCA AGG CTG AGA AC-3′ and reverse 5′-ATG GTG GTG AAG ACG CCA GT-3′.

Small interfering RNA transfection

Three different sequences of small interfering RNA (siRNA) targeting human SNAI1 (Hs_SNAI1_9785, 9786, and 9787) and those of 2 scramble control siRNAs were purchased from Sigma Aldrich Japan. The transfection methods have been previously described (17).

Statistical analysis

The statistical analyses were done using Microsoft Excel (Microsoft) both to calculate the SD and to test for statistically significant differences between the samples using a Student t test. A value $P < 0.05$ was considered statistically significant.

Results

To examine the activity of HGF-Met signaling in HCC cells, we examined the expressions of phospho-Met, Met, phospho-AKT, AKT, phospho-MAPK, and MAPK in the HepG2 and Huh7 cell lines, using Western blotting. The phosphorylation levels of Met, AKT, and MAPK were dose-dependently increased by HGF stimulation (Fig. 1A). A time-course analysis showed that the phosphorylation levels of Met, AKT, and MAPK peaked at 1 to 2 hours after HGF stimulation and gradually recovered to the baseline values at 4 hours later (Fig. 1B). These results indicated that Met signaling is actually capable of being activated in response to HGF in HCC cells.

From a morphologic aspect, the EMT is characterized by an increase in cell scattering and an elongation of the cell shape (18). To evaluate whether HGF mediates the morphologic change that is characteristic of the EMT in HCC cells, cellular morphology was examined after HGF stimulation. HGF clearly mediated both cell scattering and the elongation of the cell shape in HepG2 and Huh7 cell lines (Fig. 1C). These data indicate that HGF mediates

DOI:10.1158/1535-7163.MCT-10-0544

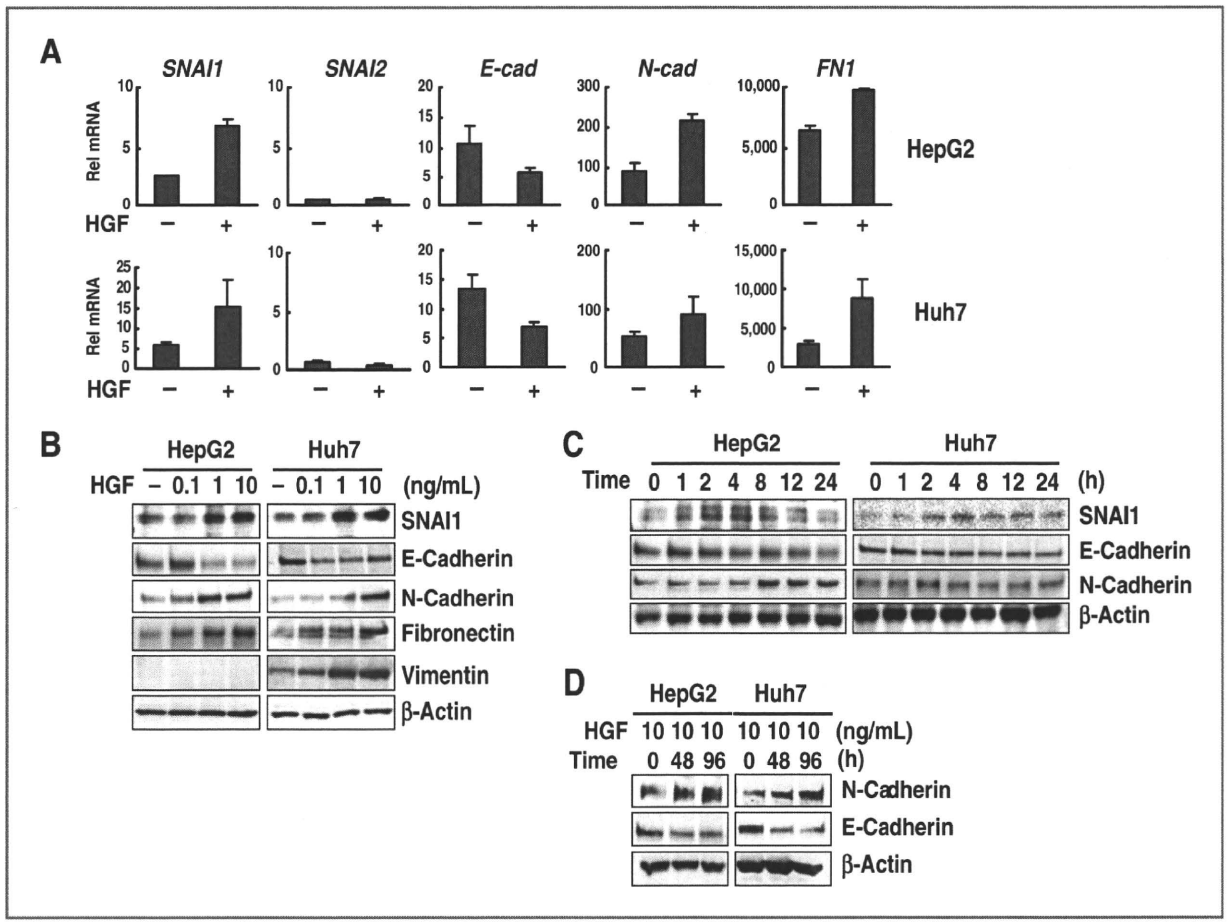

Figure 2. HGF upregulates SNAI1 expression and induces cadherin switching in HCC. A, changes in the mRNA expressions of the EMT-related genes *SNAI1/Snail*, *SNAI2/Slug*, *E-cadherin/CDH1*, *N-cadherin/CDH2*, and *fibronectin/FN1* were determined using real-time RT-PCR. The HepG2 and Huh7 cells were stimulated with or without 10 ng/mL of HGF for 2 hours (SNAI1 and SNAI2) or 48 hours (*E-cad*, *N-cad*, and *FN1*). Rel mRNA, normalized mRNA expression levels (target genes/GAPD $\times 10^4$); E-cad, E-cadherin; N-cad, N-cadherin. B, the HGF-mediated protein expression changes in SNAI1, E-cadherin, N-cadherin, fibronectin, and vimentin were determined using a Western blot analysis. The HepG2 and Huh7 cells were stimulated with HGF at the indicated dose (0, 0.1, 1, or 10 ng/mL) and collected for analysis after 4-hour stimulation for SNAI1 and 72 hours for the others. C, the cells were stimulated with 10 ng/mL of HGF for the indicated time course (0, 1, 2, 4, 8, 12, or 24 hours) and used for analysis. β-Actin was used as a loading control. D, Western blot analysis of E-cadherin and N-cadherin. The cells were stimulated with 10 ng/mL of HGF for 0, 48, and 96 hours and then analyzed.

the morphologic changes that are compatible with the induction of the EMT in HCC cell lines.

Because SNAI1 and SNAI2 are considered to be master regulators of the EMT, changes in the mRNA expression levels of EMT-related genes in response to HGF stimulation were evaluated using real-time RT-PCR (Fig. 2A). HGF stimulation upregulated SNAI1 mRNA expression by more than 2-fold, whereas the baseline expression of SNAI2 was very low compared with that of SNAI1 and did not respond to HGF in either of the HCC cell lines that were examined. Cadherin switching, which is characterized by the downregulation of E-cadherin and the upregulation of N-cadherin, is known as one of the most pivotal cellular events in the EMT (19). Cadherin switching was clearly observed on the basis of mRNA levels after HGF stimulation. The mesenchymal marker fibronectin was also upregulated (Fig. 2A).

Consistent with the mRNA changes, HGF stimulation dose-dependently upregulated the protein expression of SNAI1, N-cadherin, fibronectin, and vimentin and downregulated the expression of E-cadherin in both cell lines (Fig. 2B). Vimentin expression of HepG2 was not detected (baseline vimentin mRNA was also extremely low; data not shown). A time-course analysis showed that HGF upregulated the SNAI1 expression at 2 hours after stimulation and that the expression level recovered to the baseline value at 24 hours thereafter (Fig. 2C). Cadherin switching after HGF stimulation was observed at 8 hours later in HepG2 cells and 48 hours later in Huh7 cells (Fig. 2C and D). Generally, upregulation of SNAI1 is

DOI:10.1158/1535-7163.MCT-10-0544

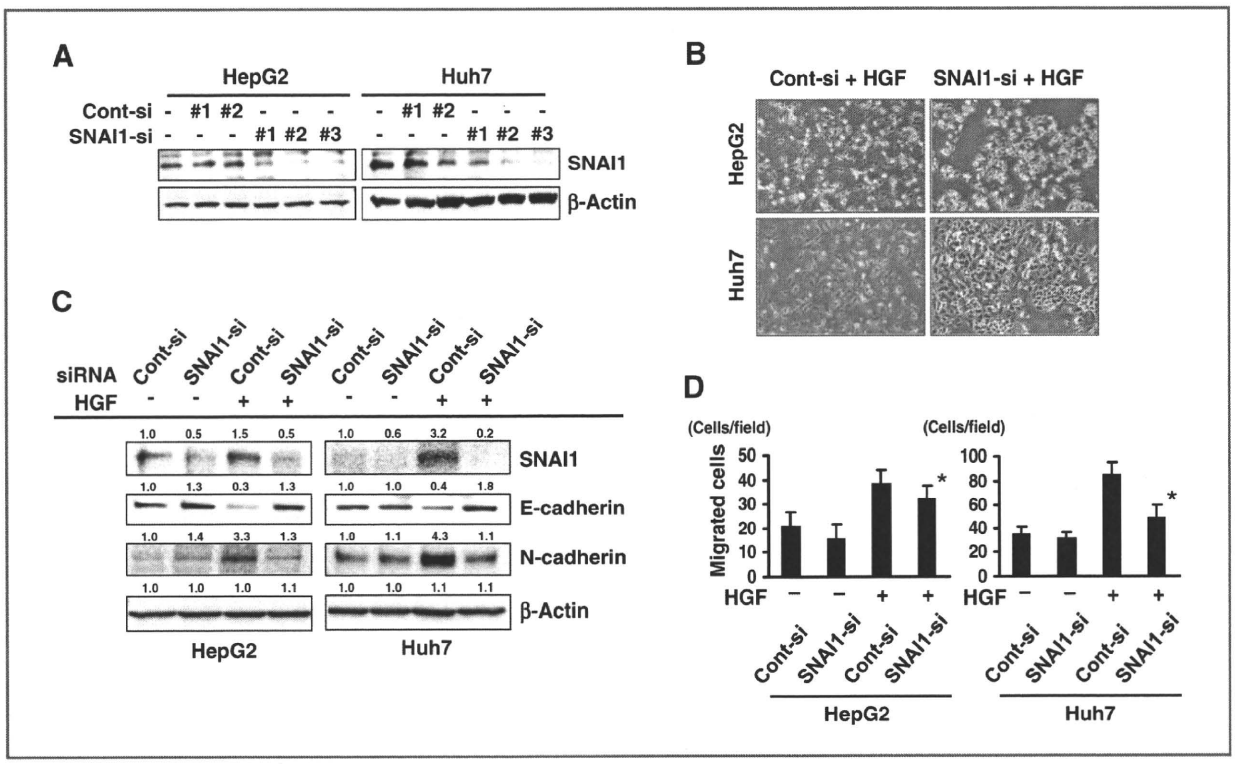

Figure 3. SNAI1 is required to induce the HGF-mediated EMT in HCC cells. A, knockdown of HGF-mediated SNAI1 expression using siRNA. Three sequences of SNAI1-siRNA (1, 2, and 3) were used. The HepG2 and Huh7 cells were treated with or without 50 nmol/L of each siRNA for 48 hours and then were stimulated with 10 ng/mL of HGF. SNAI1-siRNA #2 was effective and was used in subsequent experiments. B, SNAI1 knockdown canceled the HGF-mediated morphologic changes. The HepG2 and Huh7 cells were treated with 50 nmol/L of siRNA for 48 hours and were then stimulated with 10 ng/mL of HGF in all 4 panels. C, SNAI1 suppression by siRNA strongly canceled the HGF-mediated downregulation of E-cadherin and the upregulation of N-cadherin in both HepG2 and Huh7 cells. The cells were treated with 50 nmol/L of siRNA for 48 hours and were analyzed using a Western blot analysis. Densitometric data are shown above the Western blot. D, the siRNA knockdown of SNAI1 inhibited the HGF-mediated cellular migration. The siRNA-transfected HepG2 and Huh7 cells were evaluated using migration assay. The migration assays were conducted using the Boyden chamber methods as described in Materials and Methods. *, $P < 0.05$ (Cont-si vs. SNAI1-si with HGF); Cont-si, control-siRNA; SNAI1-si, SNAI1-targeting siRNA.

observed within few hours, but cadherin switching occurs around 24 hours later after stimulation (20, 21), consistent with our result. These results indicate that HGF meditates the induction of SNAI1, cadherin switching, and the EMT in HCC cells.

Besides SNAI1 and SNAI2, other transcription factors of several genes also have the potential to repress E-cadherin and to induce the EMT; these factors include ZEB1/TCF8, ZEB2/SMAD interacting protein 1, TWIST, E47/TCF3, and TCF4/E2-2 (6). Therefore, we examined whether SNAI1, among several EMT-inducible genes, has a central role in the HGF-mediated EMT in HCC cells. Three sequences of SNAI1-siRNA (1, 2, and 3) were used. A Western blot showed that both sequences 2 and 3 of SNAI1-siRNA completely suppressed the HGF-mediated upregulation of SNAI1 in the HepG2 and Huh7 cells (Fig. 3A); thus, the #2 SNAI1-siRNA was used in the following experiments: The siRNA knockdown of SNAI1 canceled the morphologic changes observed in HepG2 cells undergoing HGF-mediated EMT, whereas the control-siRNA did not (Fig. 3B). Similar results were obtained in Huh7 cells, indicating that SNAI1 is required for the morphologic changes observed in HGF-mediated EMT. Similarly, the siRNA knockdown of SNAI1 strongly canceled the HGF-mediated downregulation of E-cadherin and the upregulation of N-cadherin in both HepG2 and Huh7 cells (Fig. 3C). Those of mRNA expression changes were relatively correlated with the results of Western blot, except for N-cadherin in Huh7 cells (Supplementary Fig. 2A). Regarding the cellular migration, the siRNA knockdown of SNAI1 inhibited the HGF-mediated cellular migration (Fig. 3D). Collectively, these results indicate that SNAI1 is required to induce the HGF-mediated EMT in HCC cells.

In general, SNAI1 expression is regulated by ligand-receptor signal transduction through a downstream signal pathway that includes the Smad, MAPK, AKT, and GSK3 pathways (6, 22, 23). Sorafenib has been shown to inhibit RAF-MAPK signaling in HCC cells (24). Accordingly, we hypothesized that sorafenib might downregulate SNAI1 expression by inhibiting RAF-MAPK signaling, which is a unique activity of sorafenib. As

DOI:10.1158/1535-7163.MCT-10-0544

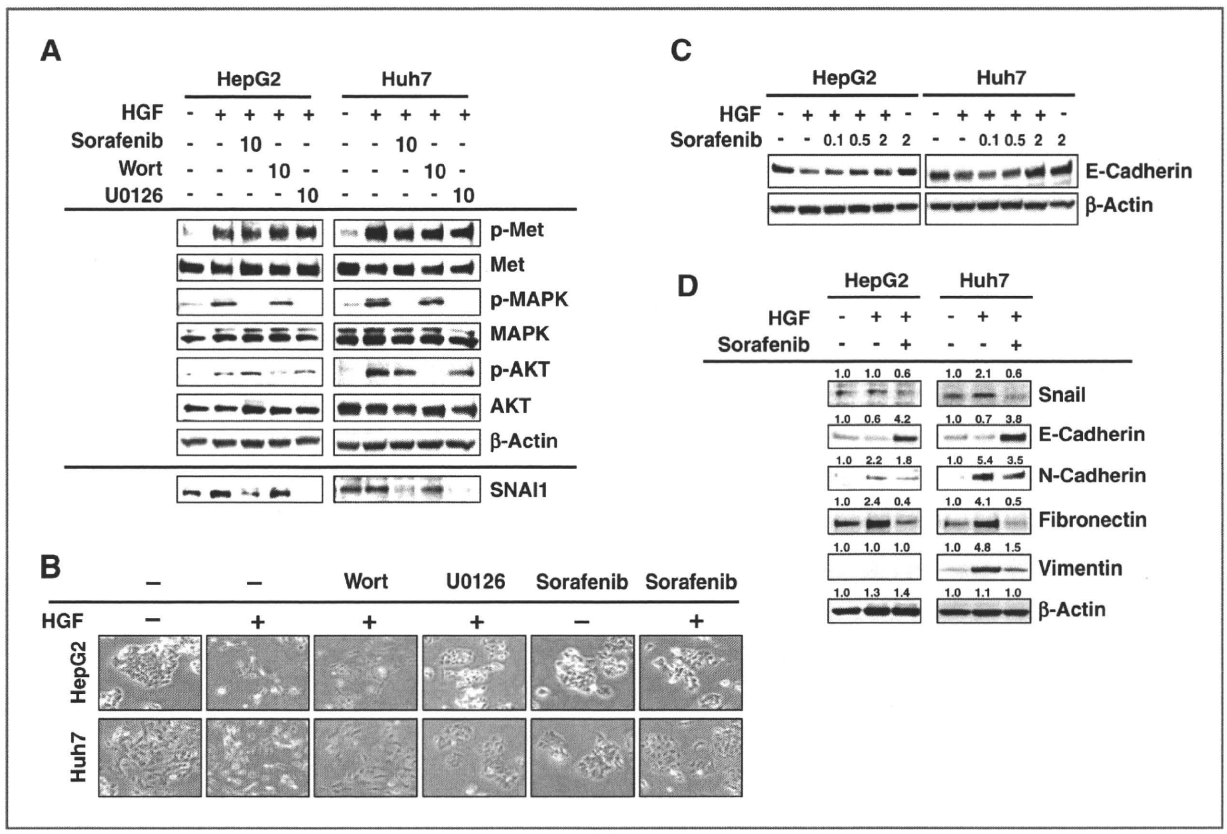

Figure 4. Sorafenib downregulates SNAI1 expression in HCC. A, as expected, sorafenib and the MEK inhibitor U0126 inhibited the HGF-mediated phosphorylation of MAPK, but the PI3K inhibitor wortmannin did not. Of note, SNAI1 expression was markedly downregulated by sorafenib and U0126. The HepG2 and Huh7 cells were exposed to 10 μmol/L of sorafenib or wortmannin or U0126 for 3 hours and were then stimulated with 10 ng/mL of HGF for 60 minutes. Wort, wortmannin. B, the HGF-mediated morphologic changes were canceled by sorafenib and U0126 but not by wortmannin in the HCC cells. The cells were exposed to sorafenib or wortmannin or U0126 for 48 hours with or without HGF (10 ng/mL) and then photographed. C, HGF-mediated downregulation of E-cadherin was canceled by sorafenib. The cells were stimulated with HGF (10 ng/mL) and treated with sorafenib at indicated concentration for 48 hours. D, HGF-mediated cadherin switching and upregulation of fibronectin and vimentin were canceled by sorafenib in the HCC cell lines. The cells were cultured with or without 2 μmol/L of sorafenib for 72 hours, with or without HGF (10 ng/mL), and then were analyzed using Western blot analysis. Densitometric data are shown above the Western blot.

expected, sorafenib and the MEK inhibitor U0126 (10 μmol/L) markedly inhibited the HGF-induced phosphorylation of MAPK, but the PI3K inhibitor wortmannin (10 μmol/L) did not. In contrast, only wortmannin inhibited the phosphorylation of AKT (Fig. 4A). Notably, SNAI1 expression was strongly downregulated by sorafenib and U0126 but not by wortmannin (Fig. 4A). These results showed that sorafenib downregulated SNAI1 expression via MAPK signaling. Meanwhile, we examined the HGF- and sorafenib-mediated expression changes of *SNAI2*, *ZEB1*, *ZEB2*, and *TWIST* using real-time RT-PCR and Western blot (Supplementary Fig. 3). Baseline and expression changes of SNAI2 and TWIST were very low compared with SNAI1, and the expression changes of ZEB1 and ZEB2 seemed not to be significant. Collectively, we considered that SNAI2, TWIST, ZEB1, and ZEB2 are not likely to be involved in the effect of HGF and sorafenib on EMT in this cell lines. Then, we examined the activity of sorafenib on HGF-mediated morphologic changes in HCC cells. HGF stimulation mediated the cell scattering and spindle-shaped changes, and these effects were clearly canceled by sorafenib and U0126, but not by wortmannin, in both HepG2 and Huh7 cells (Fig. 4B). These results were consistent with the results of Western blotting. To show whether sorafenib cancels the effect of HGF-mediated downregulation of E-cadherin, we examined the Western blot in dose–response analysis. Downregulation of E-cadherin was clearly canceled by sorafenib in a dose-dependent manner (Fig. 4C). Time-course analysis showed that HGF-mediated downregulation of E-cadherin was also canceled by sorafenib (Supplementary Fig. 4). HGF stimulation downregulated E-cadherin expression and upregulated N-cadherin, vimentin, and fibronectin in HCC cells; however, these effects were canceled by sorafenib in both HCC cell lines (Fig. 4D and Supplementary Fig. 2B). The mRNA data of N-cadherin in Huh7 cells were not correlated with protein level. These results show that sorafenib inhibits the

DOI:10.1158/1535-7163.MCT-10-0544

RAF-MAPK pathway, thereby downregulating SNAI1 and inhibiting the EMT in HCC.

Because sorafenib inhibits the HGF-mediated EMT in HCC cells, we next examined whether the inhibitory effect of sorafenib on the EMT leads to an inhibition of cellular migration in HCC cells. A scratch assay revealed that HGF stimulation increased cellular migration by about 2- fold in both HCC cell lines; however, sorafenib significantly inhibited this effect to the baseline levels (Fig. 5A). Similarly, a migration assay using the Boyden chamber method revealed that sorafenib canceled HGF-mediated cellular migration in both cell lines (Fig. 5B). These results suggest that sorafenib actually inhibits the cellular migrating phenotype of the EMT in HCC cells. The combination of migration data with siRNA and sorafenib (Fig. 3D and Fig. 5B) suggests that inhibitory effects of sorafenib on migration may be mediated by Snail downregulation in some tumors (e.g., Huh7) but not in others (e.g., HepG2). It is assumed that the inhibitory activity of sorafenib on the cellular migrating phenotype is due to its inhibitory effect of Raf-MAPK signaling pathway (Fig. 4A and B). Regarding HGF-dependent PI3K-AKT signaling pathway, wortmannin weakly inhibited the wound closure in Huh7 cells and to the same extent by sorafenib in HepG2 cells (Supplementary Fig. 5). In contrast, wortmannin has no effect on Snail levels or on HCC morphology changes (Fig. 4A and B). Collectively, we speculate that activation of HGF-dependent PI3K-AKT pathway may not be involved in SNAI1 induction or morphologic change but at least partially involved in cell migration independent of Raf-MAPK-SNAI1 signaling.

Taken together, these results indicate that sorafenib inhibits the HGF-mediated EMT, which is characterized by cadherin switching, morphologic changes, and an increase in the cellular migrating phenotype, by inhibiting Raf-MAPK signaling, resulting in the downregulation of SNAI1 in HCC cells (Fig. 6).

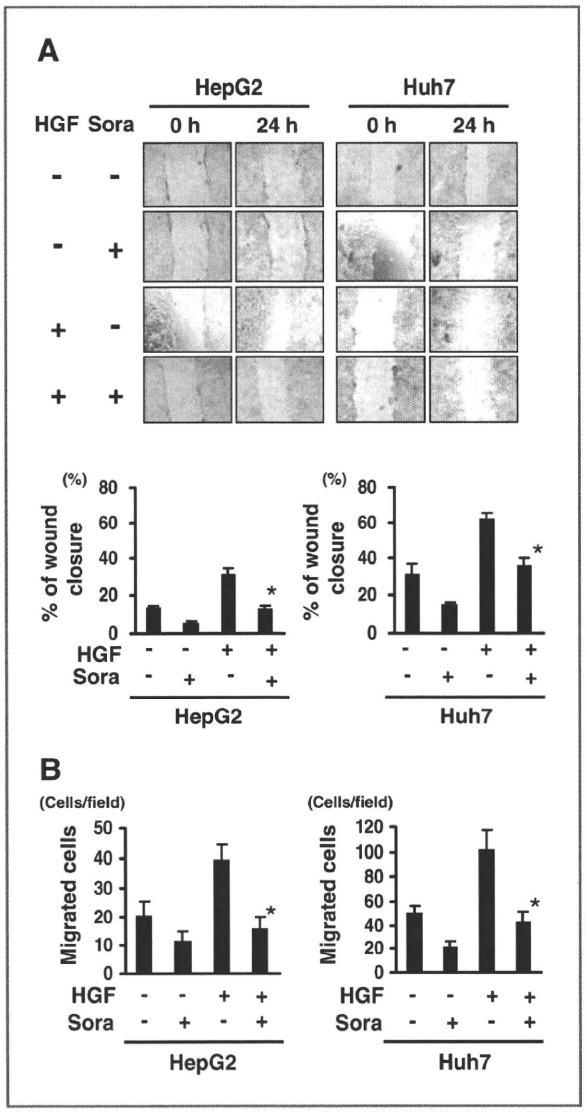

Figure 5. Sorafenib inhibits HGF-mediated cellular migration in HCC cells. A, a scratch assay revealed that HGF stimulation increased the cellular migration by about 2-fold, but sorafenib almost completely canceled the effect. The subconfluent HepG2 and Huh7 cells were scratched with a plastic pipette tip and incubated under the indicated conditions (control, 10 ng/mL of HGF; and HGF, 10 μmol/L of sorafenib). The scratch area was photographed and measured. The experiment was done in triplicate. *, sorafenib (–) versus (+), $P < 0.05$. B, migration assay using the Boyden chamber method revealed that sorafenib almost completely canceled the HGF-mediated cellular migration in both HCC cell lines. The cells were incubated under the indicated conditions: control, 10 ng/mL of HGF; and HGF, 10 μmol/L of sorafenib. *, sorafenib (–) versus (+), $P < 0.05$. Sora, sorafenib.

Discussion

Recent accumulating evidence has shown that the EMT is involved in drug sensitivity to several anticancer agents (25). Within this topic, the most intensively investigated drugs have been endothelial growth factor receptor (EGFR)–targeting drugs for the treatment of lung cancer. A clinical trial has revealed that lung cancer cells with strong E-cadherin expression exhibit a significantly longer time to progression after EGFR-TKI (tyrosine kinase inhibitor) treatment (26). Other studies on EGFR-targeting drugs have shown that mesenchymal type lung cancer cells exhibit an EMT-dependent acquisition of PDGFR, FGF receptor, and TGF-β receptor signaling pathways (27), and integrin-linked kinase is a novel target for overcoming HCC resistance to EGFR inhibition (28). Regarding sensitivity to gemcitabine, mesenchymal type cancer cells are reportedly associated with gemcitabine resistance in pancreatic cancer cells (29). The mechanism of resistance to gemcitabine has been shown to involve the activation of Notch signaling, which is mechanistically linked with the mesenchymal chemoresistance phenotype of pancreatic cancer cells (30). Thus, baseline cellular characteristics based on the EMT phenotype might be useful not only as prognostic biomarkers for a malignant phenotype but also as predictive markers

DOI:10.1158/1535-7163.MCT-10-0544

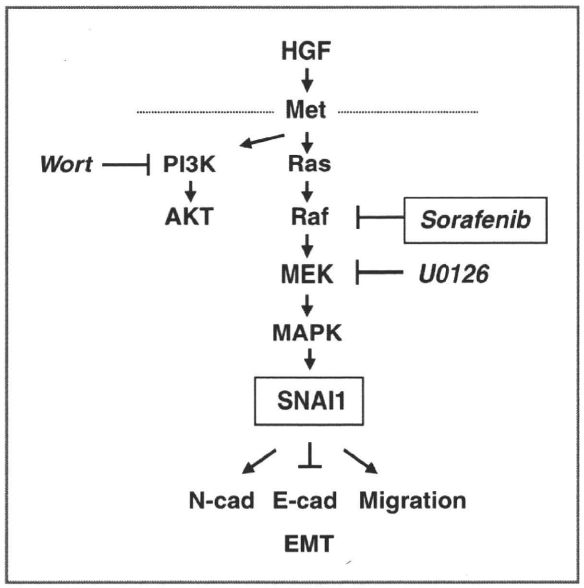

Figure 6. Diagram of the proposed mechanism by which sorafenib inhibits the EMT. Sorafenib inhibits the HGF-mediated EMT, which is characterized by morphologic changes, cadherin switching, and an increase in the cellular migrating phenotype. The anti-EMT effect of sorafenib occurs through the downregulation of SNAI1 by the inhibition of MAPK phosphorylation in HCC cells. Wort, wortmannin; N-cad, N-cadherin; E-cad, E-cadherin.

of sensitivity to anticancer agents. In this study, we focused on the signaling pathway responsible for inducing the EMT and showed that the multitarget TKI sorafenib downregulates SNAI1 by inhibiting Raf-MAPK signaling, thereby inhibiting the HGF-mediated EMT in HCC cells. Our findings may provide a novel insight into the actions of TKIs and their anti-EMT effects.

The mechanisms underlying the SNAI1-induced metastatic and aggressive phenotypes of cancer cells have recently been intensively investigated in both basic and clinical research studies. A novel aspect of the activity of SNAI1 is its involvement in immunosuppression. The SNAI1-induced EMT mediates regulatory T cells and impairs dendritic cells, accelerating cancer metastasis not only by enhancing invasion but also by inducing immunosuppression (31). A complex of histone deacetylase (HDAC) and SNAI1 plays an essential role in silencing E-cadherin (32), suggesting that the use of HDAC inhibitors to inhibit SNAI1 function might represent a promising therapeutic approach. On the other hand, large-scale clinical data on SNAI1 expression and the prognosis of patients with HCC were recently reported (33) and the overexpression of SNAI2 and/or TWIST was correlated with a worse prognosis. In contrast, no such significant differences were observed in samples that overexpressed SNAI2. The coexpression of Snail and TWIST was correlated with the worst prognosis for HCC (33). This evidence suggests that SNAI1 might be a useful therapeutic target for oncology. Our findings showed that sorafenib completely canceled the HGF-mediated SNAI1 induction in HepG2 and Huh7 cells. This activity of sorafenib, in addition to sorafenib's antiangiogenic effects, might contribute to a clinical benefit against metastatic and aggressive phenotypes in patients with HCC.

Disclosure of Potential Conflicts of Interest

No potential conflicts of interest were disclosed.

Acknowledgments

We thank Tomoko Kitayama and the staff of the Life Science Research Institute for their technical assistance.

Grant Support

This work was supported in part by the Third-Term Comprehensive 10-Year Strategy for Cancer Control and a Grant-in-Aid for Cancer Research (H20-20-9) from the Ministry of Health and Labor Scientific Research Grants.

The costs of publication of this article were defrayed in part by the payment of page charges. This article must therefore be hereby marked *advertisement* in accordance with 18 U.S.C. Section 1734 solely to indicate this fact.

Received June 9, 2010; revised October 25, 2010; accepted October 25, 2010; published online January 10, 2011

References

1. Jemal A, Murray T, Ward E, et al. Cancer statistics, 2005. CA Cancer J Clin 2005;55:10–30.
2. Yamamoto J, Kosuge T, Takayama T, et al. Recurrence of hepatocellular carcinoma after surgery. Br J Surg 1996;83:1219–22.
3. Wilhelm SM, Carter C, Tang L, et al. BAY 43-9006 exhibits broad spectrum oral antitumor activity and targets the RAF/MEK/ERK pathway and receptor tyrosine kinases involved in tumor progression and angiogenesis. Cancer Res 2004;64:7099–109.
4. Llovet JM, Ricci S, Mazzaferro V, et al.; SHARP Investigators Study Group. Sorafenib in advanced hepatocellular carcinoma. N Engl J Med 2008;359:378–90.
5. Cheng AL, Kang YK, Chen Z,, et al. Efficacy and safety of sorafenib in patients in the Asia-Pacific region with advanced hepatocellular carcinoma: a phase III randomised, double-blind, placebo-controlled trial. Lancet Oncol 2009;10:25–34.
6. Peinado H, Olmeda D, Cano A. Snail, Zeb and bHLH factors in tumour progression: an alliance against the epithelial phenotype?Nat Rev Cancer 2007;7:415–28.
7. Hugo H, Ackland ML, Blick T, et al. Epithelial-mesenchymal and mesenchymal-epithelial transitions in carcinoma progression. J Cell Physiol 2007;213:374–83.
8. Tsuji T, Ibaragi S, Hu GF. Epithelial-mesenchymal transition and cell cooperativity in metastasis. Cancer Res 2009;69:7135–9.
9. Gentile A, Trusolino L, Comoglio PM. The Met tyrosine kinase receptor in development and cancer. Cancer Metastasis Rev 2008;27:85–94.
10. Eder JP, Vande Woude GF, Boerner SA, LoRusso PM. Novel therapeutic inhibitors of the c-Met signaling pathway in cancer. Clin Cancer Res 2009;15:2207–14.
11. Yang H, Magilnick N, Noureddin M, Mato JM, Lu SC. Effect of hepatocyte growth factor on methionine adenosyltransferase genes

DOI:10.1158/1535-7163.MCT-10-0544

and growth is cell density-dependent in HepG2 cells. J Cell Physiol 2007;210:766–73.
12. Mizuguchi T, Nagayama M, Meguro M, et al. Prognostic impact of surgical complications and preoperative serum hepatocyte growth factor in hepatocellular carcinoma patients after initial hepatectomy. J Gastrointest Surg 2009;13:325–33.
13. Chau GY, Lui WY, Chi CW, et al. Significance of serum hepatocyte growth factor levels in patients with hepatocellular carcinoma undergoing hepatic resection. Eur J Surg Oncol 2008;34:333–8.
14. Yamagamim H, Moriyama M, Matsumura H, et al. Serum concentrations of human hepatocyte growth factor is a useful indicator for predicting the occurrence of hepatocellular carcinomas in C-viral chronic liver diseases. Cancer 2002;95:824–34.
15. Tanaka K, Arao T, Maegawa M, et al. SRPX2 is overexpressed in gastric cancer and promotes cellular migration and adhesion. Int J Cancer 2009;124:1072–80.
16. Matsumoto K, Arao T, Tanaka K, et al. mTOR signal and hypoxia-inducible factor-1 alpha regulate CD133 expression in cancer cells. Cancer Res 2009;69:7160–4.
17. Kaneda H, Arao T, Tanaka K, et al. FOXQ1 is overexpressed in colorectal cancer and enhances tumorigenicity and tumor growth. Cancer Res 2010;70:2053–63.
18. Lee JM, Dedhar S, Kalluri R, Thompson EW: The epithelial-mesenchymal transition: new insights in signaling, development, and disease. J Cell Biol 2006;172:973–81.
19. Wheelock MJ, Shintani Y, Maeda M, Fukumoto Y, Johnson KR. Cadherin switching. J Cell Sci 2008;121:727–35.
20. Lo HW, Hsu SC, Xia W, et al. Epidermal growth factor receptor cooperates with signal transducer and activator of transcription 3 to induce epithelial-mesenchymal transition in cancer cells via up-regulation of TWIST gene expression. Cancer Res 2007;67:9066–76.
21. Vincent T, Neve EP, Johnson JR, et al. A SNAIL1-SMAD3/4 transcriptional repressor complex promotes TGF-beta mediated epithelial-mesenchymal transition. Nat Cell Biol 2009;11:943–50.
22. Larue L, Bellacosa A. Epithelial-mesenchymal transition in development and cancer: role of phosphatidylinositol 3' kinase/AKT pathways. Oncogene 2005;24:7443–54.
23. Zavadil J, Böttinger EP. TGF-beta and epithelial-to-mesenchymal transitions. Oncogene 2005;24:5764–74.
24. Liu L, Cao Y, Chen C, et al. Sorafenib blocks the RAF/MEK/ERK pathway, inhibits tumor angiogenesis, and induces tumor cell apoptosis in hepatocellular carcinoma model PLC/PRF/5. Cancer Res 2006;66:11851–8.
25. Voulgari A, Pintzas A. Epithelial-mesenchymal transition in cancer metastasis: mechanisms, markers and strategies to overcome drug resistance in the clinic. Biochim Biophys Acta 2009;1796:75–90.
26. Yauch RL, Januario T, Eberhard DA, et al. Epithelial versus mesenchymal phenotype determines *in vitro* sensitivity and predicts clinical activity of erlotinib in lung cancer patients. Clin Cancer Res 2005; 11:8686–98.
27. Thomson S, Petti F, Sujka-Kwok I, Epstein D, Haley JD. Kinase switching in mesenchymal-like non-small cell lung cancer lines contributes to EGFR inhibitor resistance through pathway redundancy. Clin Exp Metastasis 2008;25:843–54.
28. Fuchs BC, Fujii T, Dorfman JD, et al. Epithelial-to-mesenchymal transition and integrin-linked kinase mediate sensitivity to epidermal growth factor receptor inhibition in human hepatoma cells. Cancer Res 2008;68:2391–9.
29. Arumugam T, Ramachandran V, Fournier KF, et al. Epithelial to mesenchymal transition contributes to drug resistance in pancreatic cancer. Cancer Res 2009;69:5820–8.
30. Wang Z, Li Y, Kong D, et al. Acquisition of epithelial-mesenchymal transition phenotype of gemcitabine-resistant pancreatic cancer cells is linked with activation of the notch signaling pathway. Cancer Res 2009;69:2400–7.
31. Kudo-Saito C, Shirako H, Takeuchi T, Kawakami Y. Cancer metastasis is accelerated through immunosuppression during Snail-induced EMT of cancer cells. Cancer Cell 2009;15:195–206.
32. von Burstin J, Eser S, Paul MC, et al. E-cadherin regulates metastasis of pancreatic cancer *in vivo* and is suppressed by a SNAIL/HDAC1/HDAC2 repressor complex. Gastroenterology 2009;137:361–71.
33. Yang MH, Chen CL, Chau GY, et al. Comprehensive analysis of the independent effect of Twist and Snail in promoting metastasis of hepatocellular carcinoma. Hepatology 2009;50:1464–74.

J Gastroenterol
DOI 10.1007/s00535-010-0294-5

ORIGINAL ARTICLE—LIVER, PANCREAS, AND BILIARY TRACT

The cancer stem cell marker CD133 is a predictor of the effectiveness of S1+ pegylated interferon α-2b therapy against advanced hepatocellular carcinoma

Satoru Hagiwara · Masatoshi Kudo · Kazuomi Ueshima · Hobyung Chung · Mami Yamaguchi · Masahiro Takita · Seiji Haji · Masatomo Kimura · Tokuzo Arao · Kazuto Nishio · Ah-Mee Park · Hiroshi Munakata

Received: 23 December 2009 / Accepted: 8 July 2010

Abstract
Background Combination therapy with the oral fluoropyrimidine anticancer drug S1 and interferon is reportedly effective for the treatment of advanced hepatocellular carcinoma (HCC), but selection criteria for this therapy have not been clarified. In this study, we attempted to identify factors predicting the effectiveness of this combination therapy.
Methods Pathological specimens of HCC were collected before treatment from 31 patients with advanced HCC who underwent S1+ pegylated-interferon (PEG-IFN) α-2b therapy between January 2007 and January 2009. In these pathological specimens, the expression levels of CD133, thymidylate synthase (TS), dihydropyrimidine dehydrogenase (DPD), and interferon-receptor 2 (IFNR2) proteins were determined by Western blot assay. The presence or absence of p53 gene mutations was determined by direct sequencing. The relationships between these protein expression levels and the response rate (RR), progression-free survival (PFS), and overall survival (OS) were evaluated.
Results The CD133 protein expression level was significantly lower in the responder group than in the nonresponder group. Comparing the PFS and OS between high- and low-level CD133 expression groups ($n = 13$ and 18, respectively) revealed that both parameters were significantly prolonged in the latter group. The expression levels of TS, DPD, and IFNR2 protein and the presence of p53 gene mutations did not correlate with the RR.
Conclusions CD133 was identified as a predictor of the therapeutic effect of S1+ PEG-IFN α-2b therapy against advanced HCC.

Keywords 5-Fluorouracil · Pegylated interferon · CD133 · Cancer stem cell · Hepatocellular carcinoma

S. Hagiwara · M. Kudo (✉) · K. Ueshima · H. Chung · M. Yamaguchi · M. Takita
Division of Gastroenterology and Hepatology, Department of Internal Medicine, Kinki University School of Medicine, 377-2 Ohno-Higashi, Ōsakasayama, Osaka 589-8511, Japan
e-mail: m-kudo@med.kindai.ac.jp

S. Haji
Department of Surgery, Kinki University School of Medicine, Ōsakasayama, Japan

M. Kimura
Department of Pathology, Kinki University School of Medicine, Ōsakasayama, Japan

T. Arao · K. Nishio
Department of Genome Biology, Kinki University School of Medicine, Ōsakasayama, Japan

A.-M. Park · H. Munakata
Department of Biochemistry, Kinki University School of Medicine, Ōsakasayama, Japan

Abbreviations

5FU	5-Fluorouracil
DPD	Dihydropyrimidine dehydrogenase
HCC	Hepatocellular carcinoma
IFNR2	Interferon-receptor 2
NR	Nonresponder
OS	Overall survival
PD	Progressive disease
PEG-IFN	Pegylated interferon
PFS	Progression-free survival
PR	Partial response
RR	Response rate

Published online: 04 August 2010

SD Stable disease
TS Thymidylate synthase

Introduction

Hepatocellular carcinoma (HCC) is one of the most common malignancies in Asia, including Japan [1, 2], and its prevalence has recently been increasing globally [3]. In most patients, the background of HCC is chronic hepatitis or liver cirrhosis due to hepatitis B or hepatitis C infection. Recently, HCC has increasingly been detected at relatively early stages due to the periodic follow-up of chronic liver disease patients and the development of diagnostic imaging modalities. There have been significant improvements in the treatment of patients with early HCC, and the therapeutic results have been markedly improved by site-specific treatments such as transcatheter arterial chemoembolization, percutaneous ethanol injection therapy, microwave coagulation therapy, and radiofrequency ablation, as well as hepatectomy [4–6].

However, when existing HCC is cured radically, new cancers develop due to the underlying chronic liver disorders. Treatments must then be performed alone or in combination each time a new cancer appears. Repeated treatment often leads to portal vein tumor thrombosis or distant metastasis, making standard treatments difficult to perform. Recently, the treatment efficacy and safety of the molecular targeted drug sorafenib (Nexavar; Bayer HealthCare Pharmaceuticals–Onyx Pharmaceuticals, Leverkusen, Germany) have been reported and the results placed it as a first-line drug [7]. Sorafenib is a small molecule that inhibits tumor-cell proliferation and tumor angiogenesis and increases the rate of apoptosis in a wide range of tumor models. It acts by inhibiting the serine–threonine kinases Raf-1 and B-Raf and the receptor tyrosine kinase activity of vascular endothelial growth factor receptors (VEGFRs) 1, 2, and 3 and platelet-derived growth factor receptor β (PDGFR-β). Llovet et al. [7] reported that sorafenib prolonged median survival and the time to progression by nearly 3 months in about 300 patients with advanced HCC. Although different types of molecular targeted drugs have been under development, there is no treatment option at present for the patients who fail to respond to sorafenib. Thus, second-line treatment for advanced HCC needs to be established.

The oral fluoropyrimidine anticancer drug, S1, includes the dihydropyrimidine dehydrogenase (DPD) inhibitor 5-chloro-2,4-dihydroxypyridine as a component, and this component is expected to exhibit a marked anticancer effect by preventing 5-fluorouracil (5FU) degradation [8–10]. Combination therapy with S-1 and interferon (IFN) has recently been attempted in patients with advanced HCC, and relatively satisfactory results have been reported [11–14]. However, the response rate for this therapy is limited, and the outcome deteriorates in patients resistant to it. Therefore, if the effectiveness of this therapy can be predicted in advance, unnecessary adverse effects can be avoided, and other treatments may be attempted.

We have noted some candidate proteins which may have a possible relationship with the effect of this therapy. The cancer stem-cell marker CD133 [15–18] can reportedly resist anticancer drugs through an intrinsic drug resistance mechanism [19, 20]. Thymidylate synthase (TS) and DPD are enzymes involved in 5FU metabolism, and many reports have suggested their relationship with the therapeutic effects of 5FU in lung [21] and colon cancers [22]. Furthermore, interferon-receptor 2 (IFNR2) is reported to be the most important of the receptors through which IFN acts directly on HCC [23, 24]. Apoptosis is the primary mechanism of the anticancer effect of anticancer drugs, and p53 is closely involved in apoptosis [25–27].

In the present study, we sought to identify factors predicting the effectiveness of S1+ pegylated-interferon (PEG-IFN) α-2b therapy. HCC tissue samples were collected before the therapy was started, the expression levels of CD133, TS, DPD, and IFNR2 proteins were determined by Western blot analysis, and the presence or absence of p53 gene mutations was examined by direct sequencing. We found that the expression level of CD133 was significantly correlated with the therapeutic effect. Thus, measurement of the CD133 expression level before treatment may facilitate prediction of the therapeutic effect and the avoidance of unnecessary adverse effects.

Subjects, materials, and methods

Patients

Between January 2007 and January 2009, a total of 31 patients with refractory HCC that could not be controlled by standard therapeutic modalities (transcatheter arterial chemoembolization, percutaneous ethanol injection therapy, microwave coagulation therapy, radiofrequency ablation, and hepatectomy) underwent S-1 and PEG-IFN α-2b combination therapy. Patient characteristics are shown in Table 1, with more details shown in Table 2. All pathological specimens of HCC were collected by needle biopsy.

Eligibility criteria

Eligibility criteria for the combination therapy included: (1) advanced HCC that was uncontrollable with standard treatment, or HCC with distant metastasis; (2) age <80 years; (3) an Eastern Cooperative Oncology Group performance status of 0 or 1; (4) Child–Pugh grade A; (5) encephalopathy

Table 1 Characteristics of patients treated with combination therapy of S1 and PEG-IFN α-2b

Characteristics	Number of patients
Total	31
Gender	
Male	28
Female	3
Age (years)	
Median	66
Range	30–80
Cause of disease	
HBV	10
HCV	15
Non-HBV, non-HCV	6
Child–Pugh stage	
A	31
BCLC stage	
C (advanced)	31
ECOG performance status	
0	28
1	3

PEG-IFN pegylated interferon, *HBV* hepatitis B virus, *HCV* hepatitis C virus, *BCLC* Barcelona Clinic Liver Cancer Group, *ECOG* Eastern Cooperative Oncology Group

degree 0; (6) leukocyte count >3,000 cells/mm [3]; hemoglobin level >10 g/dl and platelet count >80,000 cells/mm^3; and (7) serum creatinine <1.5 mg/dl, serum aspartate aminotransferase <200 IU/l, serum alanine aminotransferase <200 IU/l, and serum total bilirubin level <3.0 mg/dl. The diagnosis of HCC was made based on the hematoxylin–eosin staining of histopathological specimens in all patients.

Treatment regimen

After the obtaining of informed consent, 31 patients were treated with S-1 (TS1; Taiho Pharmaceutical, Tokyo, Japan) and PEG-IFN α-2b (Pegintron; Schering-Plough, Kenilworth, NJ, USA) combination therapy. S-1 was given orally at a daily dose of 80–120 mg (depending on the body surface area: <1.25 m^2: 80 mg, >1.25 to <1.5 m^2: 100 mg, <1.5 m^2: 120 mg), divided into two equal doses, from days 1 to 28. PEG-IFN α-2b was given subcutaneously at a dose of 50 μg on days 1, 8, 15, and 22. One course consisted of consecutive administration for 28 days followed by a 2-week drug-free interval. The Medical Ethics Committee of Kinki University of Medicine approved the study.

Assessment of response

Responses of HCC patients to the combination therapy were assessed by contrast-enhanced computed tomography after each course. The response was defined according to the Response Evaluation Criteria in Solid Tumours (RECIST). A partial response (PR) was defined as a minimum 30% decrease in the sum of the longest diameters of the target lesions, with the baseline sum of the longest diameters of these lesions as the reference. Progressive disease (PD) was defined as a minimum 20% increase in the sum of the longest diameters of the target lesions. Stable disease (SD) was defined as meeting neither PR nor PD criteria. When the response achieved regarding intrahepatic HCC was different from that for extrahepatic HCC, the poorer one was determined as the achieved response.

Assessment of toxicity

Blood cell counts and biochemical profiles were performed at least once every week. Adverse reactions were assessed using the National Cancer Institute-Common Toxicity Criteria (NCI-CTC, version 3).

Western blot analysis

To prepare tissue lysate, HCC tissue was homogenized with CelLytic-MT Mammalian Tissue Lysis/Extraction reagent (Sigma-Aldrich, St. Louis, MO, USA) along with 2% sodium dodecyl sulfate (SDS) and the protease inhibitor, Complete™ (Roche Diagnostics, Mannheim, Germany), and centrifuged. Equal protein amounts (8 μg) of tissue lysates were electrophoresed through a reducing SDS polyacrylamide gel and electroblotted onto a polyvinylidene difluoride (PVDF) membrane. The membrane was blocked and incubated with polyclonal IgG for TS (1/500; Taiho Pharmaceutical, Tokyo, Japan), DPD (1/3,000; Taiho Pharmaceutical), IFN-α/βR (1/500; Otsuka Pharmaceutical., Tokyo, Japan), CD133 (1/1,000; Cell Signaling Technology, Danvers, MA, USA), and β-actin (1/2,000; Sigma-Aldrich) in Can Get Signal® immunostain solution (TOYOBO, Osaka, Japan). For CD133 detection, lysis of the human colon cancer cells WiDr and DLD1 (positive and negative controls, respectively) was examined. Protein levels were detected using horseradish peroxidase (HRP)-linked secondary antibodies and the ECL-plus System (GE Healthcare, Buckinghamshire, UK).

To evaluate the signal intensity, the obtained Western blot image data were quantified using Image J software (NIH, Bethesda, MD, USA).

Immunohistochemistry

We performed immunohistochemical analysis of paraffin-embedded sections of HCC. Immunohistochemical staining was carried out with antibodies raised against CD133 (1:100), and visualized using the Dako LSAB System-HRP

Table 2 Detailed characteristics and outcomes of patients treated with combination therapy of S1 and PEG-IFN α-2b

Patient no.	Age (years)	Gender	PS	HBs-Ag	HCV-Ab	Type of intrahepatic tumor	Vascular invasion	Metastasis	Tumor grade	Prior treatment	AFP (ng/ml)		DCP (mAU/ml)		Response	Outcome
											Before	After	Before	After		
1	80	M	0	−	−	Nodular	Absence	LN	Poor[a]	OP, TACE	3	3	16	17	PR	21.2 M dead
2	70	M	0	−	−	Nodular	Presence	−	Poor	OP	6	35	5,535	60,413	PD	1.7 M dead
3	66	M	0	−	−	Nodular	Absence	Lung	Moderate[b]	OP, RFA	243	65	74	21	PR	25.4 M alive
4	61	M	0	+	−	Nodular	Absence	LN	Moderate	TACE	474	22	31	13	PR	8.1 M dead
5	62	M	0	+	−	Nodular	Absence	Lung, adrenal	Moderate	OP, HAIC	3,268	1,122	18	21	PD	1.9 M dead
6	67	M	0	+	−	Nodular	Absence	Lung	Moderate	OP, TACE	7,964	8,643	3,124	6,676	PD	1.3 M dead
7	60	M	0	−	+	Nodular	Presence	−	Poor	OP	11	13	19	37	SD	16.7 M alive
8	74	M	1	−	+	Nodular	Absence	−	Poor	OP, TACE	2,242	490	1,147	2,356	PD	3.0 M alive
9	59	F	0	+	−	Nodular	Presence	Lung	Moderate	HAIC	867	536	1,300	413	PR	7.2 M alive
10	70	M	0	−	−	Nodular	Presence	−	Moderate	−	345	26	61,319	1,024	PR	9.2 M alive
11	74	M	0	−	+	Diffuse	Presence	Adrenal	Moderate	HAIC	2,246	1,352	13,303	11,167	PR	6.6 M dead
12	60	M	0	−	+	Diffuse	Presence	−	Moderate	−	51	48	13,007	8,523	PD	3.6 M dead
13	61	M	0	+	−	Nodular	Presence	−	Moderate	−	8	9	476	209	SD	3.8 M alive
14	75	M	0	−	+	Nodular	Absence	LN	Poor	TACE	2,476	11,722	3,711	5,452	NE	0.6 M dead
15	61	M	0	+	−	Nodular	Absence	−	Poor	TACE	251	175	1,470	2,795	PD	3.8 M alive
16	30	M	0	+	−	Nodular	Presence	−	Moderate	−	114,852	79,361	195	183	PR	5.2 M alive
17	80	M	1	−	+	Diffuse	Absence	Lung, LN, bone	Moderate	−	70	106	116,140	306,800	PD	3.2 M dead
18	78	M	1	−	+	Nodular	Presence	Lung	Moderate	−	13,544	10,192	3,401	4,805	PD	2.8 M dead
19	55	M	0	−	+	Nodular	Presence	Lung, LN	Moderate	−	470	468	62,938	31,608	SD	2.0 M dead
20	35	M	0	−	+	Nodular	Presence	−	Moderate	−	91	285	44,951	58,921	PD	2.3 M dead
21	63	M	0	−	+	Nodular	Absence	−	Moderate	OP	1,140	160	412	96	PR	10.2 M alive
22	66	M	0	−	+	Nodular	Absence	−	Poor	TACE	651	872	3,231	5,890	PD	3.1 M dead
23	67	M	0	−	+	Nodular	Absence	Lung	Poor	OP	73	86	16	24	PD	3.1 M dead
24	57	M	0	−	+	Diffuse	Presence	Lung	Moderate	−	154	43	3,891	123	PR	9.5 M alive
25	65	M	0	−	+	Nodular	Absence	Lung	Moderate	OP, TACE	2,118	4,860	45,359	67,894	PD	1.9 M dead
26	51	M	0	+	−	Nodular	Absence	−	Moderate	−	1,111	3,890	240	651	PD	1.9 M dead
27	72	M	0	+	−	Nodular	Presence	Lung	Moderate	TACE	652	612	1,131	980	PD	5.6 M dead
28	74	M	0	+	−	Nodular	Presence	Lung, LN	Moderate	OP, TACE	658	890	2,418	3,168	PD	2.0 M dead
29	75	F	0	−	+	Nodular	Presence	−	Moderate	HAIC	1,153	2,789	11,456	21,998	PD	5.3 M dead
30	68	F	0	−	−	Nodular	Presence	−	Moderate	−	7	7	231	164	PR	16.2 M alive
31	58	M	0	−	−	Nodular	Presence	Lung, adrenal	Poor	TACE	86	58	14,661	11,990	SD	2.0 M alive

PS performance status, *HBs-Ag* hepatitis B surface antigen, *HCV-Ab* anti-hepatitis C virus antibody, *LN* lymph node, *TACE* transcatheter arterial chemoembolization, *RFA* radiofrequency ablation, *HAIC* hepatic arterial infusion chemotherapy using implanted port system, *AFP* alpha-fetoprotein, *DCP* des-gamma-carboxyprothrombin, *OP* operation, *M* months, *PR* partial response, *PD* progressive disease, *SD* stable disease

[a] Poorly differentiated

[b] Moderately differentiated

(Dako, Carpinteria, CA, USA). Sections were counterstained with hematoxylin.

Determination of p53 sequence

Total RNA extracted from HCC tissue using TRIZOL (Invitrogen, Carlsbad, CA, USA) was reverse-transcribed employing the Takara RNA PCR kit (AMV) Ver.3 (Takara, Tokyo, Japan). p53 was amplified using the forward primer 5′-GAGCCGCAGTCAGATCCTA-3′ and the reverse primer 5′-CAGTCTGAGTCAGGCCCTTC-3′, and nested polymerase chain reaction (PCR) was performed using the primers 5′-CCCCTCTGAGTCAGGAAACA-3′ and 5′-TTATGGCGGGAGGTAGACTG-3′. The PCR product was purified and sequenced using BigDye terminator version 3.1 cycle sequencing on an ABI 3100 DNA sequencer (Applied Biosystems, Foster City, CA, USA).

Statistical analysis

Differences between groups were examined for significance using the Mann–Whitney *U*-test and Fishers exact test where appropriate. Multivariate analysis was performed by using a logistic regression model. Cumulative survival and progression-free survival (PFS) curves were constructed using the Kaplan–Meier method and compared using the log-rank test. All the analyses described above were performed using the SPSS program (version 11.5; SPSS, Chicago, IL, USA).

Results

Response

Complete and partial responses were achieved in 0 (0%) and 10 (32.3%) of the 31 patients, respectively. The overall response rate was 32.3%. Stable disease (SD) was noted in 3 patients (9.7%), and the disease control rate (complete response + partial response + SD) was 41.9%. Progressive disease (PD) was noted in 17 patients (54.8%). One patient was excluded from the assessment of response, because the patient died of HCC rupture 17 days after the start of treatment and the computed tomography could not be performed.

Progression-free survival rate and survival assessment

The median PFS was 1.6 months (95% confidence interval [CI] 1.5–1.7 months). The cumulative PFS rates at 6, 12, and 18 months were 38, 19, and 9%, respectively.

All enrolled patients were also included in a survival assessment. Twelve patients were still alive at the end of the observation period (median 8.2 months, range 2–25.4 months), while 19 patients had died. The causes of death were tumor progression ($n = 18$) and infectious lung disease ($n = 1$). The median survival time was 5.3 months (95% CI 1.7–9.0 months). The cumulative survival rates at 6, 12, 18, and 24 months were 44, 35, 35, and 17%, respectively.

Relationship of CD133, TS, DPD, and IFNR2 protein expression levels in HCC with the anticancer effect of the combined therapy

The expression levels of CD133, TS, DPD, and IFNR2 proteins, which were candidate predictive factors for the therapeutic effect, were studied by Western blotting in all specimens. Figure 1 shows the results in five samples from the PR group and four samples from the PD group. The expression level of CD133 was low in the PR group but high in the PD group. However, no marked differences were noted in the expression levels of TS, DPD, or IFNR2 between the two groups.

Next, the relationships of the CD133, TS, DPD, and IFNR2 protein expression levels with the antitumor effect were evaluated. To compare the protein expression levels among specimens, the relative expression level was calculated by dividing the intensity of each signal on Western blotting by the signal intensity of actin, which is an internal control. The CD133 protein expression level was significantly lower in the responder group (median 0.05) than in the nonresponder group (median 0.58) group ($p = 0.005$) (Fig. 2a). In contrast, the TS, DPD, and IFNR2 protein expression levels showed no significant differences between the responder and nonresponder groups (Fig. 2b–d).

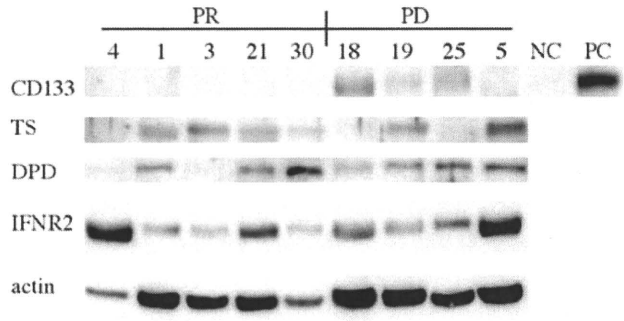

Fig. 1 Expression of CD133, thymidylate synthase (*TS*), dihydropyrimidine dehydrogenase (*DPD*), and interferon receptor 2 (*IFNR2*) as possible factors predicting the therapeutic effect in hepatocellular carcinoma (HCC). Results of Western blotting in typical cases in the partial response (*PR*) and progressive disease (*PD*) groups. For CD133, negative (DLD1) and positive (WiDr) controls were used